



Published in final edited form as:

Am J Obstet Gynecol. 2011 March ; 204(3): 254.e16–254.e28. doi:10.1016/j.ajog.2010.11.032.

CHRONIC FETAL HYPOXIA PRODUCES SELECTIVE BRAIN INJURY ASSOCIATED WITH ALTERED NITRIC OXIDE SYNTHASES

Yafeng DONG, Ph.D.^{1,2,+}, Zhiyong YU, M.D.^{1,5,+}, Yan SUN, M.D.^{1,6,+}, Hui ZHOU, M.D.¹, Josh STITES, B.S.¹, Katherine NEWELL, M.D.⁴, and Carl P. WEINER, M.D., M.B.A.^{1,2,3,+,**}

¹Department of Obstetrics and Gynecology

²Institute for Reproductive Health and Regenerative Medicine

³Department of Molecular and Integrative Physiology

⁴Department of Pathology University of Kansas School of Medicine, Kansas City, KS, 66160

⁵Department of Spine Surgery The Second Affiliated Hospital Jinan University Shenzhen, Guangdong, China

⁶Department of Obstetrics and Gynecology Third Hospital, Hebei Medical University Shijiazhuang, Hebei, China

Abstract

OBJECTIVE—The impact of chronic hypoxia on the nitric oxide synthase isoenzymes (NOSs) in specific brain structures is unknown.

STUDY DESIGN—Time-mated pregnant guinea pigs were exposed to 10.5% O₂ for 14d (HPX) or room air (NMX); L-NIL (an iNOS inhibitor, 1mg/kg/day) was administered to HPX animals for 14d (L-NIL+HPX). Fetal brains were harvested at term. Multi-labeled immunofluorescence was used to generate a brain injury map. Laser capture microdissection and quantitative PCR were applied and cell injury markers, apoptosis activation, neuron loss, total NO, and the levels of individual NOSs quantified.

RESULTS—Chronic hypoxia causes selective fetal brain injury rather than globally. Injury is associated with differentially affected NO synthases in both neurons and glial cells, with iNOS up regulated at all injury sites. L-NIL attenuated the injury despite continued hypoxia.

CONCLUSIONS—These studies demonstrate chronic hypoxia selectively injures the fetal brain in part by the differential regulation of NOSs in an anatomic and cell specific manner.

Keywords

chronic hypoxia; fetal brain injury; cerebral palsy; growth restriction; IUGR; nitric oxide synthases; selective iNOS inhibition

© 2010 Mosby, Inc. All rights reserved.

**Corresponding author: K.E. Krantz Professor and Chair Department of Obstetrics and Gynecology 3901 Rainbow Blvd, MS2028 Kansas City, KS 66160 Tel: 913-588-6239 Fax: 913-588-3298 cweiner@kumc.edu.

⁺Contribute equally

Publisher's Disclaimer: This is a PDF file of an unedited manuscript that has been accepted for publication. As a service to our customers we are providing this early version of the manuscript. The manuscript will undergo copyediting, typesetting, and review of the resulting proof before it is published in its final citable form. Please note that during the production process errors may be discovered which could affect the content, and all legal disclaimers that apply to the journal pertain.

INTRODUCTION

Fetal brain abnormalities (whether developmental or acquired) contribute to numerous postnatal disorders ranging from learning disability to severe neurologic handicap¹. On the severe end, cerebral palsy (CP) complicates 1.5-6/1000 deliveries and is independently associated with spontaneous preterm birth, maternal-perinatal infection-inflammation and intrauterine growth restriction (IUGR), a frequent surrogate for chronic fetal hypoxia². The fact that other central nervous system (CNS) abnormalities are common in CP suggests CP is a phenotype more than a specific injury. The estimated lifetime excess cost of CP and CP associated disorders per individual exceeds \$1.5 million^{3,4}. The proportion of CP generally attributed to acute intrapartum ischemia-reperfusion approximates 15% and reflects the assumption that the intrapartum event was causative. Yet many affected newborns have other antecedents of CP including prematurity, chorioamnionitis, IUGR or structural malformation⁵⁻⁷, and the combination of intrauterine asphyxia and inflammation dramatically increases the risk of CP⁸. In one of the few studies of the presumably chronically hypoxic fetal brain, 43% of perinates who either died *in utero* or shortly after birth had evidence of placental vascular problems such as funisitis and antemortem brain injury including gliosis and neuronal necrosis⁹. Such changes could not result from an intrapartum event since there was inadequate elapsed time before death to account for the findings. This body of information suggests acute intrapartum ischemia-reperfusion in isolation is an uncommon cause of CP. It also suggests inflammation (funisitis and gliosis) is part of the human phenotype, and consistent with the clinical fact that early delivery of the chronically hypoxic fetus does not improve neurodevelopmental outcome⁷.

The associations between intrauterine infection / inflammation and developmental brain injury have been extensively studied. Interleukin (IL) -1 and IL-6 are central to the pathogenesis of white matter injury mediated by intrauterine infection^{10,11}. Tumor necrosis factor (TNF)- α in the setting of intrauterine infection is associated with neonatal intraventricular hemorrhage, periventricular leukomalacia and the subsequent development of CP^{10,12}. Thus, it is reasonable to speculate that inflammation plays a role in the pathogenesis of perinatal brain injury. We demonstrated that chronic hypoxia increases IL-6 and TNF- α in fetal blood of guinea pig, fulfilling the diagnostic criteria in humans for fetal inflammatory response syndrome¹³. This inflammatory response is highly associated with both spontaneous preterm birth and subsequent neurodevelopmental compromise^{14,15}. Chronic hypoxia also increased the expression of these cytokines in multiple fetal organs including the brain¹³. And while there is extensive evidence linking acute perinatal ischemia¹⁶ to proinflammatory cytokine and reactive oxygen species (ROS) generation¹⁷, no such association has been identified for the more common clinical condition associated with neurodevelopmental compromise, chronic fetal hypoxia due to placental dysfunction.

Nitric oxide (NO) is involved in diverse physiological and pathological processes. A decade ago, we documented that chronic hypoxia altered the expression of endothelial and neuronal nitric oxide synthase (e or nNOS) in the ovine fetal cerebrum¹⁸. Our finding that chronic fetal hypoxia decreased eNOS but increased nNOS suggested the normal fetal response to chronic hypoxia could be actually maladaptive since the lack of eNOS derived NO might prolong an episode of ischemia while the increased nNOS could prove cytotoxic by increasing the release of excitatory amino acids. Recently, Haynes et al applied immunocytochemistry to archived human tissue and observed a significant increase in the density of iNOS-expressing cells in the cerebral white matter of cases with periventricular leukomalacia compared to control¹⁹. This study supports an important role for iNOS-induced nitrosative stress in the reactive/inflammatory component of periventricular leukomalacia (PVL). Herein, we test the hypothesis that fetal brain injury resulting from

chronic hypoxia is selective rather than global, and that the anatomic sites of injury reflect altered expression of one or more NOS isoform.

MATERIALS AND METHODS

Animal Model

Female Duncan-Hartley guinea pigs (term~65 d) were time-mated, and dams randomly assigned to either room air (approximately 21% O₂, NMX, n=6) or to an environmental chamber containing 10.5% O₂ for 14d (HPX, n=6) beginning day 46-49 (about 0.7 gestation). Normal guinea pig chow was provided without restriction. On day 60-64, a hysterotomy was aseptically performed while dams respired spontaneously (ketamine [80mg/kg] and xylazine [1mg/kg]), and the fetal brains collected into either formalin as described below for histological study or frozen in liquid nitrogen for gene quantification. Only the presenting pup was studied. We have shown in the past that the hypoxic dams gain weight normally throughout gestation, labor and deliver without event, and that the pups are reduced in size but have increased hemoglobin and hypoxia inducible factor measurements²⁰⁻²³. In order to test the role of iNOS on fetal brain injury, L-N6-(1-Iminoethyl)-lysine (L-NIL), a selective pharmacological inhibitor of iNOS known to cross the placenta was administered to HPX animals in their drinking water (1mg/kg/d, L-NIL+HPX, n=6) for 14 days.

Fetal Brain Frozen Section Preparation

The fresh fetal whole brains from NMX (n=6), HPX animals (n=6), or L-NIL+HPX (n=6) were removed and fixed in 4% paraformaldehyde overnight at 4°C, cryoprotected in 30% sucrose at 4°C for 2-3 day until no longer buoyant, and then embedded in optimal cutting temperature compound (OCT) for sectioning. Five sets of coronal mirror sections were prepared for DAB-based immunostaining, multi labeled fluorescence immunostaining, Terminal deoxynucleotidyl transferase dUTP Nick End Labeling (TUNEL) staining, Nissl staining and Laser Capture Microdissection (LCM). The coronal sections were made at the interaural level of 6.72mm to 5.40 mm (Bregma: from -2.28 mm to -3.60mm) of the fetal brain, cut on a cryostat at 8µm thickness with each mirror section cut at 10µm intervals before being stored at -20°C for later study. These sections did not include the cerebellum and brainstem which will be studied in the future.

Fetal Brain Cell Injury Detection by Immunohistochemistry

The antibodies are described in Table 1 (Injury Index Mapping section).

The first set mirror slides were immunostained with specific antibodies against Activating Transcription Factor 3 (ATF3), a marker of neuronal injury^{24, 25} and Glial Fibrillary Acidic Protein (GFAP), a marker of glial activation²⁶. The Universal Dako LSAB immunohistochemistry staining assay (Dako North America, CA) was used for signal detection. The fetal brain sections were incubated at room temperature in 3% hydrogen peroxide for 5min and then rinsed with PBS. Primary antibodies (Table 1) to ATF3 (mouse, 1:50, Sigma, MO) and GFAP (mouse, 1:100, Sigma, MO) were applied overnight at 4°C, labeled with streptavidin-biotin and developed in 3,3'-Diaminobenzidine (DAB) to produce brown staining. Hematoxylin was used as a counterstain. Histological quantification was performed as described subsequently.

Co-localization of NOS Isoforms with Cell Injury by Multi labeled Immunofluorescence Histochemistry Staining

The second set of mirror slides were used for protein co-localization studies by multi label immune-fluorescence histochemistry with the primary antibodies described in Table 1

(ATF3 and NOSs Co-localization section). For ATF3 co-localization, β -tubulin III and GFAP were used to label neurons and glial cells respectively. The primary antibodies for ATF3 and GFAP, or ATF3 and β -tubulin III were applied to the slides and incubated overnight at 4°C with gentle agitation. The sections then were washed 5× for 10min in phosphate buffered saline (PBS), incubated in darkness with the specific secondary antibodies and rinsed 5× for 10min in PBS before being mounted with DAPI and coverslipped. Protein expression was identified under the appropriate specific fluorescence wavelengths.

For the NOS co-localization studies, the injured areas were first detected using either ATF3 or GFAP, followed by nNOS or iNOS (primary antibodies and specific secondary antibodies described in Table 1, NOSs Co-localization section). The staining procedure was the same as described as above. The primary antibodies were omitted as a negative control.

Detection of Apoptotic Cells

The third set of mirror slides were used to identify apoptotic cells based on the presence of DNA strand breaks using TUNEL. Frozen fetal brain sections were used for TUNEL staining by the Fluorescent in Situ Cell Death Detection Kit (Roche, IN) per the manufacturer's instructions. The negative control was generated by using Label Solution without terminal transferase. Positive control slides were generated by treating sections with recombinant DNase I. Each stained section was examined by fluorescent microscopy and TUNEL-positive cells in the fetal brain were quantified as previously reported²⁷.

Neuron Loss Identification by Nissl staining

The fourth set of mirror slides were used to quantify neuronal density using Nissl staining with Cresyl violet²⁸. Frozen slides were air dried for 1h, stained in Cresyl violet solution (0.1% Cresyl violet) for 5min, rinsed in distilled water, differentiated in 95% ethyl alcohol for 15min, dehydrated in 100% alcohol for 5min twice, cleared in xylene for 5min twice, and then mounted by resinous medium for the quantification.

Histological Injury Marker Quantification and Reconstruction

Histological quantification was performed as previously described²⁷. We selected six (5) animal from each group (NMX, HPX, and L-NIL+HPX). Five (5) slides were selected randomly from each animal, and then 5 injured areas were randomly selected from each slide. The grading of ATF3, GFAP and TUNEL staining intensity was determined in a blind fashion employing a 1-4 scale: weak (+), positive stained cells in $\leq 25\%$ of the surface area; medium (++) , positive cells in $> 25\%$ but $< 50\%$ of the surface area; strong (+++), positive cells in $\geq 50\%$ but $\leq 70\%$ of the surface; very strong (++++), positive cells in $\geq 70\%$ of the surface. For Nissl staining, the number of stained neurons was quantified using the Stereo Investigator 8.0 system. Neuronal density was defined as the mean total number of neurons per mm².

The locations of the injured cells marked by ATF3, GFAP and TUNEL were reconstructed from the immunostained/TUNEL stained mirror sections with the aid of a Zeiss microscope and a Nikon fluorescent microscope. The counts of positively stained cells were performed as described above, and the locations of GFAP, ATF3 and TUNEL positive cells projected onto a schematic representation of the brain coronal section as previous published²⁹.

Laser Capture Microdissection (LCM)

The fifth and final set of mirror slides was used for laser capture microdissection (LCM). The areas of injury identified by ATF3, GFAP or TUNEL labeling in the first four sets of mirror sections were selectively excised using LCM. The position of anatomical landmarks

(3rd ventricle, hippocampus, and cortex) was visually projected onto the sections for LCM from hematoxylin stained images. LCM was performed using the Veritas Microdissection Instrument on the unstained frozen section adjacent to the mirror section processed for either immuno or TUNEL staining. The regions of the unstained section that corresponded to boundaries of the injured brain areas were dissected under a 4× objective into CapSure Macro caps, and the LCM samples then used for gene quantification. Laser settings varied as needed from 50-75 mW (power), 1,500 – 3,500 ms (duration) and 200-250 mV (intensity).

Quantitative Reverse Transcriptase Polymerase Chain Reaction (Q-rtPCR)

Injury index genes (ATF3, GFAP and Bax [a marker for apoptosis]) and the three NOS isoforms (nNOS, iNOS and eNOS) mRNA expressions were quantified by SYBR Green I labeled (BioRad Laboratories, Hercules, CA) quantitative real time PCR (Q-rtPCR) using mRNA extracted from LCM samples and whole fetal brain as indicated. Total RNA was isolated (RNeasy Mini Kit and RNase-Free DNase Set, Qiagen, Valencia, CA) and reverse-transcribed (Sensiscript RT Kits, Qiagen, Valencia, CA). The primer sequence for each gene target was based on prior publications^{30,31,32,33}. PCR parameters (iCycler iQ Real-time PCR Detection System (BioRad Laboratories, Hercules, CA) consisted of an initial denaturation at 95°C for 180sec, followed by 40 cycles at 95°C for 30sec, annealing at 60°C for 25sec, extension at 72°C for 30sec, and 1 cycle at 72°C for 7min. A melt analysis was performed to confirm the specificity of the PCR amplification. PCR efficiency was demonstrated by the standard curve slope. Target gene mRNA was quantified by the delta-delta CT (2-DDCt) method and normalized to the 18S subunit of rRNA (Applied Biosystems, Foster City, CA).

Total NO Product Measurement

Nitrite/nitrate levels (NO_2^- and NO^-) were measured using a commercial assay (Fluorometric NO Assay, EMD Biosciences, CA). Whole frozen fetal brains from NMX, HPX and L-NIL+HPX animals were homogenized, centrifuged at $16,000 \times g$ for 20min, and the supernatant filtered through a 10KD cutoff filter at $14,000 \times g$ for 1h. Enzyme cofactors and nitrate reductase were added to each sample based on the manufacturer's instructions. The fluorescing reagent, DAN (2,3-diaminonaphthotriazole) was then added to the samples and loaded onto 96 well plates which were read with a Biotek Synergy HT Multi-Detection microtiter plate reader at the following settings: excitation wavelength: 360-365 nm; emission wave-length: 430-450nm.

Statistical Analyses

All results are presented as the mean \pm SEM. Comparisons between the control and study groups were calculated by t-test or ANOVA as indicated. A value of $P < 0.05$ was considered to indicate statistically significant differences between or among groups.

RESULTS

Chronic Fetal Hypoxia Results in Selective Brain Injury

Chronic fetal hypoxia over the last 30% of gestation produced selective rather than global brain injury as reflected by specific locations of increased ATF3, the development of gliosis, apoptosis and decreased neuronal density (Figure 1-3, table 2). The major structures affected were the cerebral cortex, hippocampus, and thalamic nuclei including hypothalamic nuclei (Figure 1, 2 and Table 2). The impact of chronic hypoxia was widespread in the cerebral cortex without area concentration. In contrast, significant injury in the hippocampus was seen only in the cingulum, orices layer, CA1, CA2, and CA3; the impact on CA3 was notable (Figure 2, Table 2).

In the thalamic nuclei, chronic hypoxia increased the studied markers of injury in the laterodorsal thalamic nuclei, post thalamic nuclei, ventral thalamic nuclei, paraventricular thalamic nuclei, mediodorsal thalamic nuclei, central thalamic nuclei, and reuniens thalamic nuclei. The degree of injury as reflected in the intensity of marker staining was greatest in the reuniens thalamic nuclei, central thalamic nuclei, ventral thalamic nuclei, and laterodorsal thalamus nuclei. In hypothalamic nuclei, injury was greatest in the dorsomedial hypothalamic nuclei, ventromedial hypothalamic nuclei and lateral hypothalamus (Figure 2, Table 2).

We also studied the expression of the injury markers at their mRNA levels. ATF3, GFAP and Bax mRNA expressions were quantified by Q-rtPCR, and each gene was significantly increased by chronic hypoxia in both whole brain samples and individually in LCM-derived biopsy samples from cerebral cortex, hippocampus and thalamus nuclei (Figure 4). Thus, chronic hypoxia mediated fetal brain damage increases the studied injury markers at both the mRNA and protein levels in an anatomically selective manner.

Chronic Hypoxia Affects NOS Isoforms Differently

Chronic hypoxia increased total nitric oxide (NO) in whole fetal brain (Figure 10), with both nNOS and iNOS expressions increased, but eNOS decreased (Figure 5 A). However, the impact of chronic hypoxia on the expression of the three NO synthases varied by the isoform and the structure injured. In hippocampus, iNOS expression was increased, eNOS decreased, and nNOS unchanged (Figure 5 B). In cerebral cortex, only iNOS expression was increased; there were no significant affect of chronic hypoxia on either nNOS or eNOS (Figure 5 C). Lastly, in the thalamus including hypothalamic nuclei, nNOS and iNOS expressions were both increased by chronic hypoxia while eNOS was unchanged (Figure 5 D).

Co-localization of iNOS, nNOS with the studied injury markers was sought using double fluorescent staining techniques by region and cell type. iNOS and/or nNOS co-localized to ATF3 and/or GFAP positive cells in cerebral cortex, hippocampus and thalamus nuclei regions. Figure 6 illustrates the thalamic nuclei region where hypoxia increased iNOS in thalamic nuclei (A1 vs. B1 and C1 vs. D1), neurons stained by ATF3 (A2 vs. B2) and glial cells stained by GFAP (C2 vs. D2). The expression of iNOS co-localizes with both ATF3 and GFAP positive cells (B3 and D3).

Figure 7 demonstrates that hypoxia increases nNOS (A1 vs. B1 and C1 vs. D1), ATF3 (A2 vs. B2), GFAP (C2 vs. D2), and that nNOS co-localizes with both ATF3 and GFAP positive cells (B3 and D3).

ATF3 is Present in Both Fetal Neuron and Glial Cells after Chronic Hypoxia

Neurons and glial cells were labeled by Tubulin III (red) and GFAP (green), respectively. Chronic hypoxia significantly decreased neuronal density (Figure 8: A1 vs. B1), but induced the development of gliosis (Figure 8: C1 vs. D1). ATF3 was significantly up-regulated by chronic hypoxia in neurons identified by Tubulin III (yellow color in Figure 5: A3 and B3) as expected. However, ATF3 also co-localized with the activated fetal glial cells as stained by GFAP (Figure 8: C3 vs. D3).

L-NIL Attenuates Fetal Brain Injury from Chronic Hypoxia

The selective inhibition of iNOS using L-NIL was confirmed as L-NIL did not affect nNOS and eNOS activation during chronic hypoxia (Figure 9, n=6), but it did significantly reduce iNOS suggesting a feedback loop on transcription. Total NO was blunt by L-NIL (Figure 10, n=6) illustrating their major contribution of iNOS to the excess NO generated in the brain of chronically hypoxic fetuses. As might be expected based on the afore findings, L-NIL

significantly blunted the impact of chronic hypoxia on the studied brain injury genes (ATF3, GFAP and Bax) (Figure 11). Lastly, and most importantly, L-NIL prevented the loss of neurons due to chronic hypoxia as illustrated in the hippocampus.

COMMENT

The present investigation demonstrates that chronic fetal hypoxia over the last 30% of pregnancy generates, in addition to IUGR, a pattern of fetal brain injury consistent with that observed in human perinates. The sites of injury, cerebral cortex, hippocampus, and thalamic and hypothalamic nuclei are selective rather than global and involve both gray and white matter. Injury is associated with alterations in each of the NO synthases with the induction of iNOS being ubiquitous which is also consistent with the limited human study¹⁹.

Fetal hypoxia has duration, gestational age and selective anatomic and cellular effects. Observations of the human fetal brain suggest acute ischemia-reperfusion at term pregnancy preferentially affects the neuron, while in the preterm brain it is the white matter that is preferential injured including gliosis³⁴. However, the impact of hypoxia is never exclusively on the white or gray matter. The pre and immature oligodendrocytes that characterize the preterm, periventricular white matter of the human fetus seem particularly susceptible to hypoxia-ischemic injury, and that injury is associated with limited capacity to resist oxidative stress³⁵. We have previously shown that the human preterm fetus has limited free radical scavenging capacity³⁶, suggesting the potential for enhanced free radical toxicity exists both prior to and shortly after preterm birth.

The clinical presentation of the resulting brain injury also differs between acute and chronic hypoxia. Signs of encephalopathy after an episode of acute ischemia-reperfusion typically begin during the early neonatal period. In contrast, early symptoms are relatively uncommon after chronic hypoxial injury. Mixed phenotypes also occur.

Animal models of acute fetal ischemic hypoxia in early in gestation produce neuronal death including Purkinje cells in the cerebellum, pyramidal cells in the hippocampus and cortical neurons³⁷. There is no resulting IUGR. The same insult can also generate diffuse white matter injury including gliosis and cystic lesions in the periventricular region as often seen in children with CP. An acute ischemic insult late in the pregnancy of sheep preferentially affects fetal gray matter of the cerebral cortex and striatum³⁸.

In contrast to acute hypoxia, animal models of chronic hypoxia are associated with IUGR. The growth of neural processes and synaptogenesis are affected globally^{39, 40}. Neuronal loss and ventriculomegaly are also associated with chronic hypoxia⁴¹. Chronic hypoxia in fetal sheep significantly delays the migration of cells from the germinal to the pyramidal layers of the CA1 region in the ventral hippocampus decreasing pyramidal neuron density by 35% decrease. It also reduces the area of Purkinje cell dendrite arborization in the cerebellum by 20%, and significantly decreases white matter area³⁹.

Reactive oxygen and nitrogen species play important roles in the initiation of apoptotic mechanisms and in mitochondrial permeability transition. The immature brain is particularly susceptible to free radical injury since many of the scavenging systems are as yet undeveloped and because the availability of iron for the catalytic formation of free radicals is high. Oxidative stress is an early feature of acute cerebral ischemia and experimental studies targeting the formation of free radicals reveal various degrees of protection after perinatal insult by their inhibition. For example, we have previously demonstrated that treating the dam with N acetyl cysteine prevents the development of a fetal inflammatory response after the administration of lipopolysaccharide⁴². Oxidative stress-regulated release

of pro-apoptotic factors from mitochondria appears to play an important role in the immature brain. And while neurons are considered more vulnerable to free radical damage than glial cells, oligodendrocyte progenitors and immature oligodendrocytes in very premature infants are selectively vulnerable to antioxidants depletion and free radical attack⁴³.

We have previously shown that this model of chronic fetal hypoxia generates inflammatory response in fetal multiple organs including the brain^{13, 44}. This response is unique to the fetus as the brain of the dam is unaffected. In the present study, we map for the first time the geography of fetal brain injury resulting from chronic fetal hypoxia and reveal specific injury to neuronal and glial cells at locations analogous to those reported in children with CP. This map provides a reference point for the future study of chronic hypoxia induced fetal brain injury and the impact of therapeutic interventions to ameliorate or prevent the injury. Further, we link for the first time the injury from chronic hypoxia to specific changes in NOS isoenzymes.

iNOS was expressed by both neuronal and glial cells in all injured areas. Using the iNOS selective inhibitor, L-NIL, we demonstrated that most of the hypoxia induced increase in total NO was a reflection of excess iNOS activity, and that inhibiting iNOS blunted or eliminated the expected increases in the injury indices (ATF3, GFAP and Bax). Increased iNOS results in excess oxygen free radical production which the immature cells of the perinatal brain are poorly equipped to scavenge⁴⁵. As a result of iNOS inhibition, the loss of neurons prevented despite continued fetal hypoxia. This finding raises the potential of antenatal therapy. Unfortunately, iNOS of unknown role is ubiquitously expressed in the human placental bed and periodically in various fetal organs. However, pharmacologic blockade elsewhere along the pathophysiological pathway may prove practical.

We also found that chronic hypoxia decreased eNOS in the hippocampus and increased nNOS in the thalamus (again, in both neuronal and glial cells). This pattern of adaptation would indeed exacerbate the impact of any additional, acute ischemic-reperfusion event (e.g. umbilical cord compression) that might occur during the pregnancy or labor converting a chronic injury with a subclinical phenotype into one with a clinically detectable phenotype. These common events would not otherwise produce clinically significant injury to a healthy fetus, but in the chronically hypoxic fetus with NOS adaptations, they constitute a 'second hit' to the brain and explain in part the association between CP 'due' to an acute intrapartum event with co-existing IUGR. It might also explain the synergistic relationship between IUGR and infection/inflammation noted epidemiologically as the diagnosis of infection is usually based on evidence of histological evidence of inflammation rather than the identification of bacteria. Even with the application of PCR, bacteria are detectable in no more than half of all cases⁴⁶. The NOS maladapted perinatal brain, especially if preterm would then suffer a 'third hit' when challenged by the obligatory increase in oxygen free radicals generated immediately after birth when arterial oxygen suddenly increases before the induction of adequate scavenging capacity. The 'second' and 'third hits' to the perinate could explain how a short infusion of magnesium sulfate could reduce the risk of CP by about 40%^{47,48} should the magnesium interfere with or ameliorate the inflammatory response or enhance the neonatal ability to quench free radicals. The efficacy of magnesium sulfate suggests that the 'second hit' and 'third hit' to the perinatal brain peripartal is responsible for the disease phenotype in some 40% of CP cases. In the remaining 60%, the degree of antenatal injury is already sufficient that a disease phenotype is unavoidable even with optimal perinatal management.

We have previously demonstrated that the fetal response to chronic hypoxia differs from the maternal response. For example, NOS protein expression is differently altered by hypoxia in

fetal and adult heart⁴⁹. The current investigation reveals another difference in the response to hypoxia between fetus and adult. While ATF3 in adults is considered a selective marker for neuronal injury, we find that both the neuronal and glial cells produce ATF3 when injured by hypoxia beginning at 0.7 gestation. ATF3 is a member of the mammalian activation transcription factor/cAMP responsive element-binding (CREB) protein family of transcription factors. Multiple transcript variants encoding two different isoforms are reported⁵⁰. The longer isoform represses rather than activates transcription from promoters with ATF binding elements. The shorter isoform (deltaZip2) lacks the leucine zipper protein-dimerization motif and does not bind DNA. It stimulates transcription presumably by sequestering inhibitory co-factors away from the promoter. ATF3 interacts with C-jun, DNA damage-inducible transcript 3 and P53^{50, 51}. In prior study, we demonstrated chronic fetal hypoxia increases P-53 expression in the hippocampus in proportion to the level of hypoxia⁴⁴. We cannot exclude the possibility of a unique fetal splice variant that would explain the differences in expression between adult and fetal glial cells.

Clearly, the regions injured in association with chronic hypoxia could account for much of the spectrum of abnormalities associated with perinatal brain injury. For example, the roles of the cerebral cortex include the initiation of movement. The hippocampus is important for learning and memory. The thalamus, which is located between the cerebral cortex and midbrain both in terms of location and neurological connections, is important for relaying sensation, special sense and motor signals to the cerebral cortex, along with the regulation of consciousness, sleep and alertness. Virtually every sensory system except smell has a corresponding thalamic nucleus that receives sensory signals that links to an associated primary cortical area. Loss of thalamic neurons could have significant impact on refined function; profound thalamic damage can produce coma. A core function of the hypothalamus is to link the nervous and endocrine systems through the pituitary; it synthesizes and secretes neurohormones that in turn stimulate or inhibit the secretion of pituitary hormones. The hypothalamus also controls body temperature, hunger, thirst, fatigue, and circadian cycles.

In conclusion, chronic fetal hypoxia over the last 30% of the guinea pig gestation produces an anatomically selective and cell specific pattern of brain injury characterized by neuronal loss and a reactive gliosis. All injured sites display the induction of iNOS and in some locales, nNOS is increased and or eNOS decreased. The impact of chronic hypoxia on the NO synthases is an example of an adaptive response that in terms of the birth process is maladaptive, increasing the susceptibility of the perinatal brain to what would normally be limited but well tolerated episodes of acute ischemia reperfusion.

Acknowledgments

This study described was supported in part by the PHS (R01 HL049041-13, CPW), CDC (DP00187-5, CPW) and NICHD (RO3 HD062734, Y Dong).

REFERENCES

1. Nelson KB, Ellenberg JH. Antecedents of cerebral palsy. Multivariate analysis of risk. *N Engl J Med*. Jul 10; 1986 315(2):81–86. [PubMed: 3724803]
2. Paneth N, Hong T, Korzeniewski S. The descriptive epidemiology of cerebral palsy. *Clin Perinatol*. Jun; 2006 33(2):251–267. [PubMed: 16765723]
3. Kruse M, Michelsen SI, Flachs EM, Bronnum-Hansen H, Madsen M, Uldall P. Lifetime costs of cerebral palsy. *Dev Med Child Neurol*. Aug; 2009 51(8):622–628. [PubMed: 19416329]
4. Economic costs associated with mental retardation, cerebral palsy, hearing loss, and vision impairment--United States, 2003. *MMWR Morb Mortal Wkly Rep*. Jan 30; 2004 53(3):57–59. [PubMed: 14749614]

5. Grether JK, Nelson KB. Maternal infection and cerebral palsy in infants of normal birth weight. *Jama*. Jul 16; 1997 278(3):207–211. [PubMed: 9218666]
6. Wu YW, Croen LA, Shah SJ, Newman TB, Najjar DV. Cerebral palsy in a term population: risk factors and neuroimaging findings. *Pediatrics*. Aug; 2006 118(2):690–697. [PubMed: 16882824]
7. Wu YW, Escobar GJ, Grether JK, Croen LA, Greene JD, Newman TB. Chorioamnionitis and cerebral palsy in term and near-term infants. *Jama*. Nov 26; 2003 290(20):2677–2684. [PubMed: 14645309]
8. Nelson KB, Grether JK. Potentially asphyxiating conditions and spastic cerebral palsy in infants of normal birth weight. *Am J Obstet Gynecol*. Aug; 1998 179(2):507–513. [PubMed: 9731861]
9. Grafe MR. The correlation of prenatal brain damage with placental pathology. *J Neuropathol Exp Neurol*. Jul; 1994 53(4):407–415. [PubMed: 8021715]
10. Rezaie P, Dean A. Periventricular leukomalacia, inflammation and white matter lesions within the developing nervous system. *Neuropathology*. Sep; 2002 22(3):106–132. [PubMed: 12416551]
11. Yu HM, Yuan TM, Gu WZ, Li JP. Expression of glial fibrillary acidic protein in developing rat brain after intrauterine infection. *Neuropathology*. Jun; 2004 24(2):136–143. [PubMed: 15139591]
12. Gibson CS, MacLennan AH, Goldwater PN, Dekker GA. Antenatal causes of cerebral palsy: associations between inherited thrombophilias, viral and bacterial infection, and inherited susceptibility to infection. *Obstet Gynecol Surv*. Mar; 2003 58(3):209–220. [PubMed: 12612461]
13. Yafeng D, Weijian H, Jiaxue W, Weiner CP. Chronic hypoxemia absent bacterial infection is one cause of the fetal inflammatory response syndrome (FIRS). *Reprod Sci*. Jul; 2009 16(7):650–656. [PubMed: 19351964]
14. Stoll BJ, Hansen NI, Adams-Chapman I, et al. Neurodevelopmental and growth impairment among extremely low-birth-weight infants with neonatal infection. *Jama*. Nov 17; 2004 292(19):2357–2365. [PubMed: 15547163]
15. Bashiri A, Burstein E, Mazor M. Cerebral palsy and fetal inflammatory response syndrome: a review. *J Perinat Med*. 2006; 34(1):5–12. [PubMed: 16489880]
16. Vannucci RC, Vannucci SJ. A model of perinatal hypoxic-ischemic brain damage. *Ann N Y Acad Sci*. Dec 19.1997 835:234–249. [PubMed: 9616778]
17. van den Tweel ER, Nijboer C, Kavelaars A, Heijnen CJ, Groenendaal F, van Bel F. Expression of nitric oxide synthase isoforms and nitrotyrosine formation after hypoxia-ischemia in the neonatal rat brain. *J Neuroimmunol*. Oct; 2005 167(1-2):64–71. [PubMed: 16112751]
18. Aguan K, Murotsuki J, Gagnon R, Thompson LP, Weiner CP. Effect of chronic hypoxemia on the regulation of nitric-oxide synthase in the fetal sheep brain. *Brain Res Dev Brain Res*. Dec 7; 1998 111(2):271–277.
19. Haynes RL, Folkerth RD, Trachtenberg FL, Volpe JJ, Kinney HC. Nitrosative stress and inducible nitric oxide synthase expression in periventricular leukomalacia. *Acta Neuropathol*. Sep; 2009 118(3):391–399. [PubMed: 19415311]
20. Dong Y, Thompson LP. Differential expression of endothelial nitric oxide synthase in coronary and cardiac tissue in hypoxic fetal guinea pig hearts. *J Soc Gynecol Investig*. Oct; 2006 13(7):483–490.
21. Thompson LP, Aguan K, Zhou H. Chronic hypoxia inhibits contraction of fetal arteries by increased endothelium-derived nitric oxide and prostaglandin synthesis. *J Soc Gynecol Investig*. Dec; 2004 11(8):511–520.
22. Thompson LP, Aguan K, Pinkas G, Weiner CP. Chronic hypoxia increases the NO contribution of acetylcholine vasodilation of the fetal guinea pig heart. *Am J Physiol Regul Integr Comp Physiol*. Nov; 2000 279(5):R1813–1820. [PubMed: 11049865]
23. Thompson LP, Weiner CP. Effects of acute and chronic hypoxia on nitric oxide-mediated relaxation of fetal guinea pig arteries. *Am J Obstet Gynecol*. Jul; 1999 181(1):105–111. [PubMed: 10411804]
24. Takeda M, Kato H, Takamiya A, Yoshida A, Kiyama H. Injury-specific expression of activating transcription factor-3 in retinal ganglion cells and its colocalized expression with phosphorylated c-Jun. *Invest Ophthalmol Vis Sci*. Aug; 2000 41(9):2412–2421. [PubMed: 10937548]

25. Mayumi-Matsuda K, Kojima S, Nakayama T, Suzuki H, Sakata T. Scanning gene expression during neuronal cell death evoked by nerve growth factor depletion. *Biochim Biophys Acta*. Dec 23; 1999 1489(2-3):293–302. [PubMed: 10673030]
26. Nakase T, Sohl G, Theis M, Willecke K, Naus CC. Increased apoptosis and inflammation after focal brain ischemia in mice lacking connexin43 in astrocytes. *Am J Pathol*. Jun; 2004 164(6): 2067–2075. [PubMed: 15161641]
27. Ota A, Ikeda T, Ikenoue T, Toshimori K. Sequence of neuronal responses assessed by immunohistochemistry in the newborn rat brain after hypoxia-ischemia. *Am J Obstet Gynecol*. Sep; 1997 177(3):519–526. [PubMed: 9322617]
28. Wahlsten D, Colbourne F, Pleus R. A robust, efficient and flexible method for staining myelinated axons in blocks of brain tissue. *J Neurosci Methods*. Mar 15; 2003 123(2):207–214. [PubMed: 12606069]
29. Homberg U, Brandl C, Clynen E, Schoofs L, Veenstra JA. Mas-allatotropin/Lom-AG-myotropin I immunostaining in the brain of the locust, *Schistocerca gregaria*. *Cell Tissue Res*. Nov; 2004 318(2):439–457. [PubMed: 15480799]
30. Maallem S, Wierinckx A, Lachuer J, Kwon MH, Tappaz ML. Gene expression profiling in brain following acute systemic hypertonicity: novel genes possibly involved in osmoadaptation. *J Neurochem*. May; 2008 105(4):1198–1211. [PubMed: 18194432]
31. Sandhir R, Onyszchuk G, Berman NE. Exacerbated glial response in the aged mouse hippocampus following controlled cortical impact injury. *Exp Neurol*. Oct; 2008 213(2):372–380. [PubMed: 18692046]
32. Lyahyai J, Bolea R, Serrano C, et al. Correlation between Bax overexpression and prion deposition in medulla oblongata from natural scrapie without evidence of apoptosis. *Acta Neuropathol*. Oct; 2006 112(4):451–460. [PubMed: 16804709]
33. Aguilera P, Chanez-Cardenas ME, Florian-Sanchez E, et al. Time-related changes in constitutive and inducible nitric oxide synthases in the rat striatum in a model of Huntington's disease. *Neurotoxicology*. Nov; 2007 28(6):1200–1207. [PubMed: 17850874]
34. Volpe JJ. Neurobiology of periventricular leukomalacia in the premature infant. *Pediatr Res*. Nov; 2001 50(5):553–562. [PubMed: 11641446]
35. Back T. Pathophysiology of the ischemic penumbra--revision of a concept. *Cell Mol Neurobiol*. Dec; 1998 18(6):621–638. [PubMed: 9876870]
36. Buhimschi IA, Buhimschi CS, Pupkin M, Weiner CP. Beneficial impact of term labor: nonenzymatic antioxidant reserve in the human fetus. *Am J Obstet Gynecol*. Jul; 2003 189(1): 181–188. [PubMed: 12861160]
37. Rees S, Stringer M, Just Y, Hooper SB, Harding R. The vulnerability of the fetal sheep brain to hypoxemia at mid-gestation. *Brain Res Dev Brain Res*. Nov 12; 1997 103(2):103–118.
38. Loeliger M, Watson CS, Reynolds JD, et al. Extracellular glutamate levels and neuropathology in cerebral white matter following repeated umbilical cord occlusion in the near term fetal sheep. *Neuroscience*. 2003; 116(3):705–714. [PubMed: 12573713]
39. Rees S, Harding R. The effects of intrauterine growth retardation on the development of the Purkinje cell dendritic tree in the cerebellar cortex of fetal sheep: a note on the ontogeny of the Purkinje cell. *Int J Dev Neurosci*. 1988; 6(5):461–469. [PubMed: 2462330]
40. Dieni S, Rees S. Dendritic morphology is altered in hippocampal neurons following prenatal compromise. *J Neurobiol*. Apr; 2003 55(1):41–52. [PubMed: 12605458]
41. Mallard EC, Rehn A, Rees S, Tolcos M, Copolov D. Ventriculomegaly and reduced hippocampal volume following intrauterine growth-restriction: implications for the aetiology of schizophrenia. *Schizophr Res*. Nov 9; 1999 40(1):11–21. [PubMed: 10541002]
42. Buhimschi IA, Buhimschi CS, Weiner CP. Protective effect of N-acetylcysteine against fetal death and preterm labor induced by maternal inflammation. *Am J Obstet Gynecol*. Jan; 2003 188(1): 203–208. [PubMed: 12548218]
43. Blomgren K, Hagberg H. Free radicals, mitochondria, and hypoxia-ischemia in the developing brain. *Free Radic Biol Med*. Feb 1; 2006 40(3):388–397. [PubMed: 16443153]

44. Rong G, Weijian H, Yafeng D, Zhiyong Y, Stites J, Weiner CP. Brain injury caused by chronic fetal hypoxemia is mediated by inflammatory cascade activation. *Reprod Sci.* Jun; 17(6):540–548. [PubMed: 20360591]
45. Kifle Y, Monnier J, Chesrown SE, Raizada MK, Nick HS. Regulation of the manganese superoxide dismutase and inducible nitric oxide synthase gene in rat neuronal and glial cells. *J Neurochem.* May; 1996 66(5):2128–2135. [PubMed: 8780045]
46. Digiulio DB, Romero R, Kusanovic JP, et al. Prevalence and Diversity of Microbes in the Amniotic Fluid, the Fetal Inflammatory Response, and Pregnancy Outcome in Women with Preterm Pre-Labor Rupture of Membranes. *Am J Reprod Immunol.* Mar 21.
47. Rouse DJ, Hirtz DG, Thom E, et al. A randomized, controlled trial of magnesium sulfate for the prevention of cerebral palsy. *N Engl J Med.* Aug 28; 2008 359(9):895–905. [PubMed: 18753646]
48. Doyle LW, Crowther CA, Middleton P, Marret S, Rouse D. Magnesium sulphate for women at risk of preterm birth for neuroprotection of the fetus. *Cochrane Database Syst Rev.* 2009; (1) CD004661.
49. Thompson LP, Dong Y. Chronic hypoxia decreases endothelial nitric oxide synthase protein expression in fetal guinea pig hearts. *J Soc Gynecol Investig.* Sep; 2005 12(6):388–395.
50. Nobori K, Ito H, Tamamori-Adachi M, et al. ATF3 inhibits doxorubicin-induced apoptosis in cardiac myocytes: a novel cardioprotective role of ATF3. *J Mol Cell Cardiol.* Oct; 2002 34(10): 1387–1397. [PubMed: 12392999]
51. Einbond LS, Su T, Wu HA, et al. The growth inhibitory effect of actein on human breast cancer cells is associated with activation of stress response pathways. *Int J Cancer.* Nov 1; 2007 121(9): 2073–2083. [PubMed: 17621630]

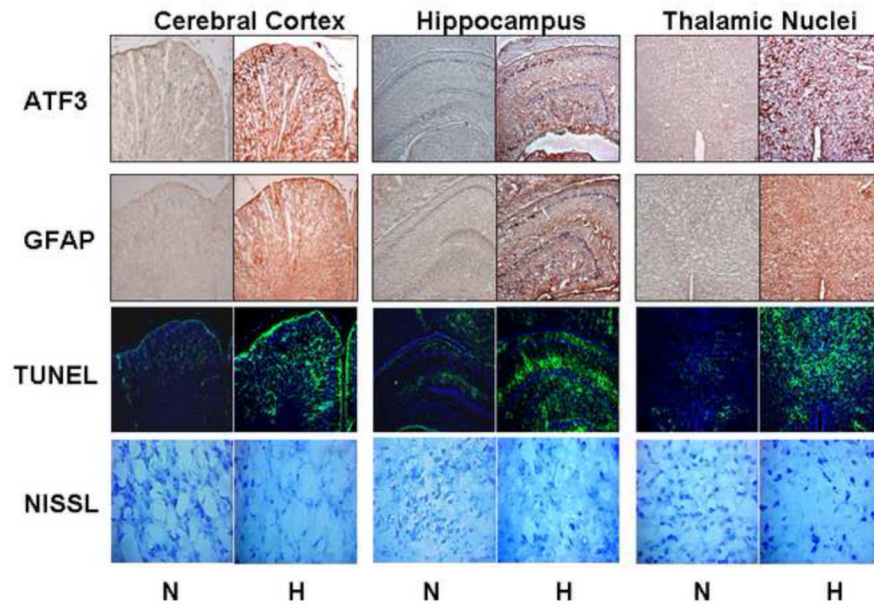


Figure 1. Chronic Fetal Hypoxia Results in Selective Anatomic Brain Injury

Sample photomicrographs from mirror image coronal sections at the interaural level of 6.72mm to 5.40 mm (Bregma: from -2.28 mm to -3.60mm) including cerebral cortex, hippocampus, and thalamic nuclei from hypoxic (n=6) and control fetuses (n=6) stained for ATF3 (10x), GFAB (10x), TUNEL (10x), and Nissl (20x). Chronic hypoxia (10.5% O₂ over the last 30% of gestation) visually increases ATF3, GFAB and TUNEL staining with an accompanying decrease in neuronal density.

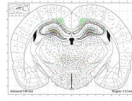


Figure 2. MAP of the Fetal Brain Injury Associated with Chronic Hypoxia

Injured areas in the mirror sections were selected at the interaural level of 6.72mm to 5.40 mm (Bregma: from -2.28 mm to -3.60mm) were reconstructed based on quantification of immunostaining and TUNEL staining. The quantification of ATF3, GFAP and TUNEL were projected onto the standard coronal section. Chronic fetal hypoxia increased ATF3 (red), GFAP (green), and TUNEL (blue) staining specifically in cerebral cortex, hippocampus, and thalamic / hypothalamic nuclei. In cortex, the damage was widely distributed, while in hippocampus, the injury was greatest in cingulum, orices layer, and CA1, CA2, CA3 layers. In thalamic nuclei, the injury was greatest in the reuniens, central, ventral, and laterodorsal thalamic nuclei. The injury markers were also up regulated in the dorsomedial and ventromedial hypothalamic nuclei and lateral hypothalamus.

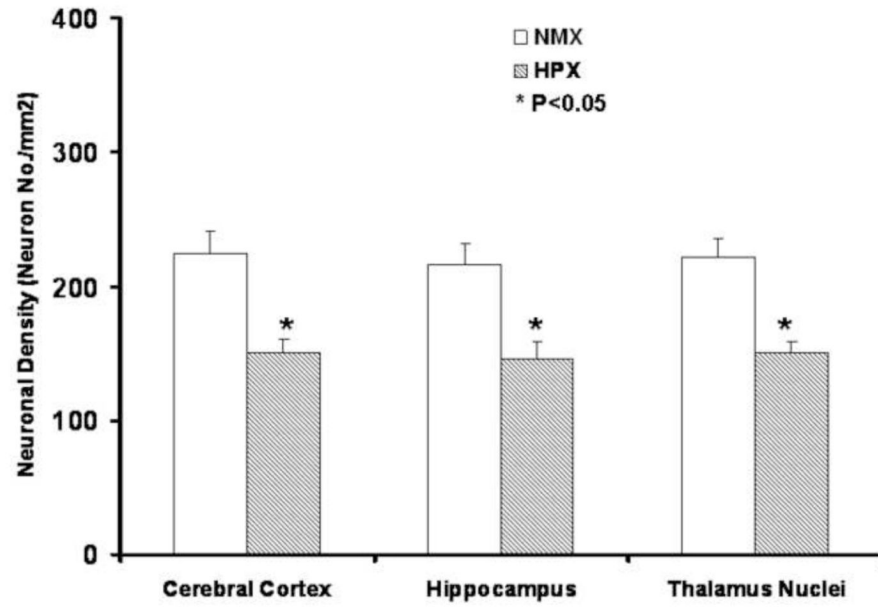


Figure 3. Neuronal Loss is Associated with Chronic Fetal Hypoxia

Neural cell density expressed as the total Nissl staining cells/mm². Five areas were randomly selected from each slide, digitally photographed, and neuronal density quantified using the Stereo Investigator 8.0 system. Chronic hypoxia over the latter 30% of gestation reduced neuronal density by some 20% in fetal cerebral cortex, hippocampus and thalamus nuclei.

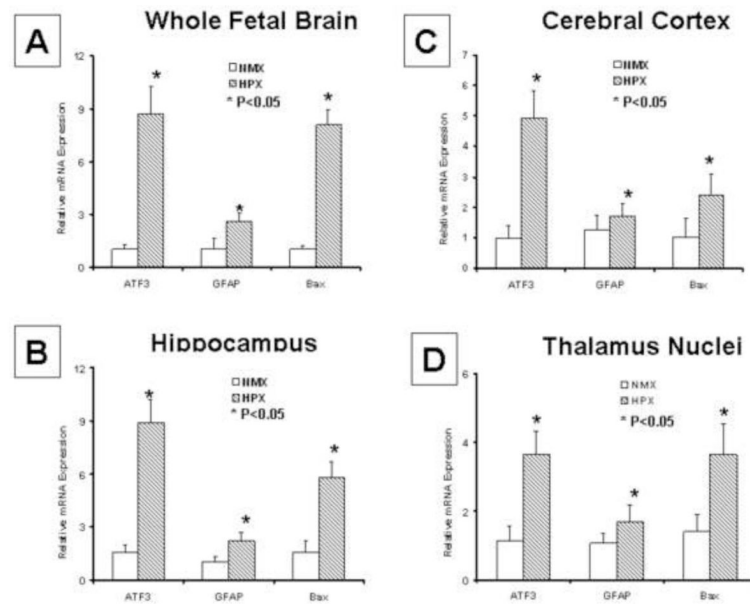


Figure 4. mRNA Expression of Brain Injury Indices is Increased by Chronic Fetal Hypoxia Cerebral cortex, hippocampus and thalamus nuclei were selectively biopsied at the sites of injury discovered in the brain slices using laser capture microdissection (LCM) and ATF3, GFAP and Bax mRNA expressions measured by Q-rtPCR. The mRNA expression for each injury marker was up regulated by chronic hypoxia (n=6, p<0.05) in both whole brain samples and at each of the LCM biopsied sites. These results, combined with the immunostaining findings demonstrate that chronic hypoxia selectively injures the fetal brain and that both mRNA and protein levels are increased.

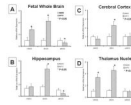


Figure 5. Chronic Hypoxia Differentially Impacts NO Synthases in a Manner that Reflects the Anatomic Location

NOS isoform mRNA was measured by Q-rtPCR in whole brain and at sites of injury in cerebral cortex, hippocampus and thalamus biopsied using LCM. In fetal whole brain (panel A), both nNOS and iNOS expressions were increased, but eNOS decreased. However, the impact of chronic hypoxia on NOS isoform expression varied by site. iNOS was increased, eNOS was decreased, and nNOS unchanged in hippocampus (panel B). In cerebral cortex, only iNOS was increased (panel C). In thalamus, nNOS and iNOS were both increased by chronic hypoxia but eNOS was unchanged (panel D).

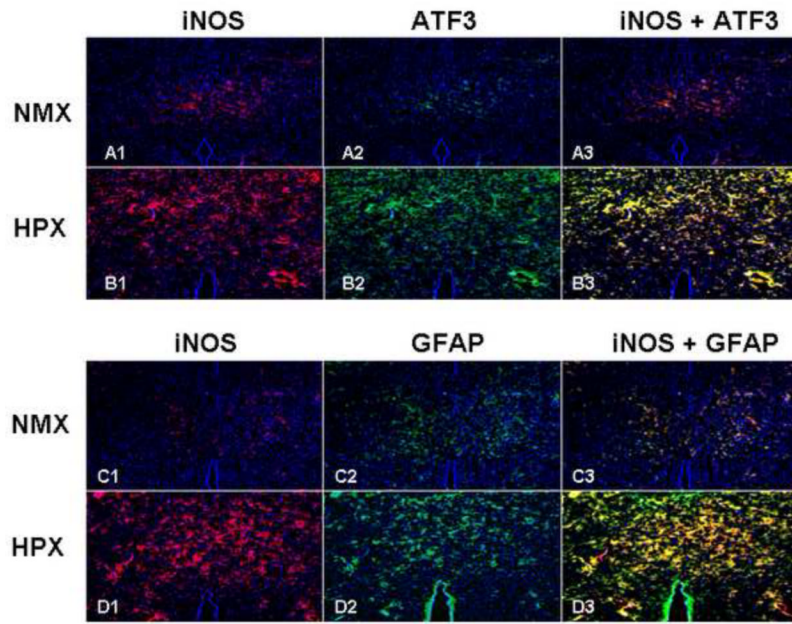


Figure 6. iNOS Co-localizes with Markers of Brain Injury

Co-localization of iNOS and injury markers was sought using double fluorescent staining techniques (cross section hippocampus, ATF3 and GFAP, 10x). Chronic hypoxia increased iNOS (panels A1 vs. B1 and C1 vs. D1), ATF3 (panels A2 vs. B2) and GFAP panels (C2 vs. D2). iNOS co-localized with both ATF3 and GFAP positive cells (panels B3 and D3).

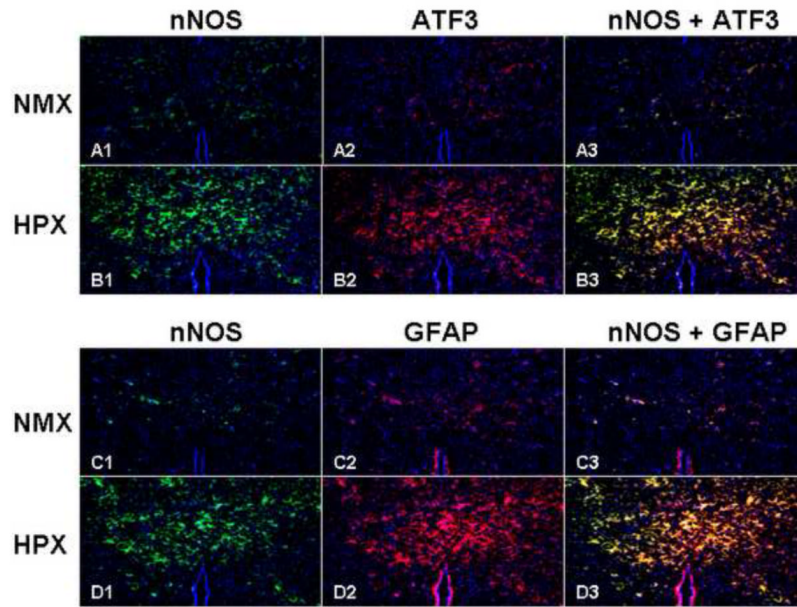


Figure 7. nNOS Co-localizes with Markers of Brain Injury

Co-localization of nNOS and injury markers was sought using double fluorescent staining techniques (cross section hippocampus, ATF3 and GFAP, 10x). Chronic hypoxia increased nNOS (panels A1 vs. B1 and C1 vs. D1), ATF3 (panels A2 vs. B2), GFAP (panels C2 vs. D2). nNOS co-localized with both ATF3 and GFAP positive cells (panels B3 and D3).

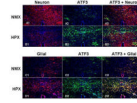


Figure 8. ATF3 is Present in Injured Fetal Neuronal and Glial Cells During Chronic Hypoxia
 Neuronal and glial cells were selectively stained for Tubulin III and GFAP, respectively (cross section hippocampus, 10x). Chronic fetal hypoxia increased ATF3 (panels A2 vs. B2, C2 vs. D2). Chronic hypoxia decreased neuronal density (panels A1 vs. B1). GFAP was activated by chronic hypoxia indicating the development of gliosis (panels C1 vs. D1). However, and in contrast to adult studies, ATF3 was not unique to neurons (A3 vs. B3), but also co-localized to glial cell after chronic hypoxia (panels C3 vs. D3).

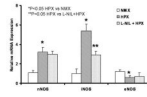


Figure 9. L-NIL Selectively Inhibits iNOS in Fetal Brain During Chronic Hypoxia
 NOS isoforms mRNA expression was quantified by Real-time PCR using the fetal whole brain tissue (n=6). nNOS and iNOS but eNOS was up-regulated significantly by chronic hypoxia and unaffected by L-NIL; only iNOS was attenuated by L-NIL.

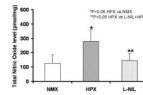


Figure 10. L-NIL Blunts the Increase in Total NO in Fetal Brain Secondary to Chronic Hypoxia Whole fetal brain total NO (NO_2^- and NO^-) was increased by chronic fetal hypoxia (HPX, n=6) vs. control animals (NMX, n=6), but significantly decreased in L-NIL treatment group vs. HPX.

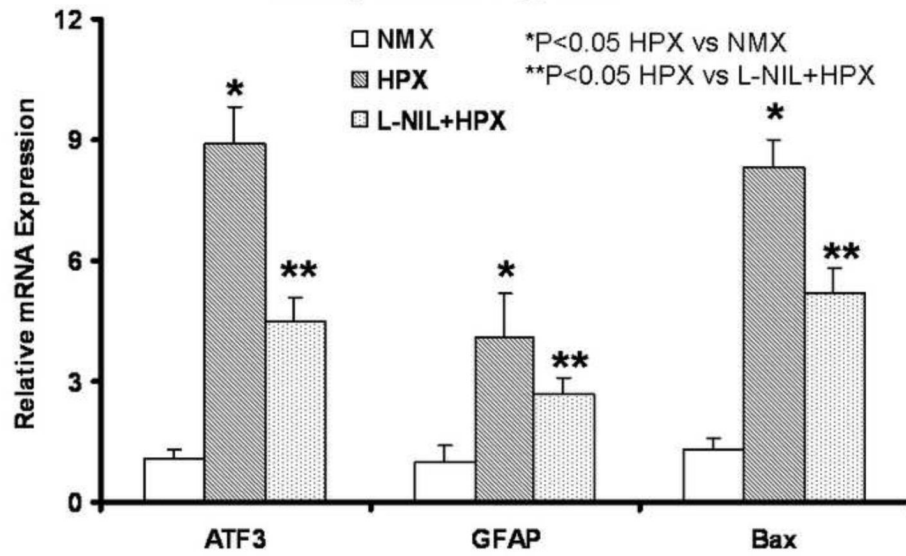


Figure 11. L-NIL Reduces Indices of Brain Injury During Chronic Hypoxia

ATF3, GFAP, and Bax were applied as indices of brain injury (n=6). Chronic hypoxia up regulated the expression of each; L-NIL attenuates the effect of unopposed chronic hypoxia.

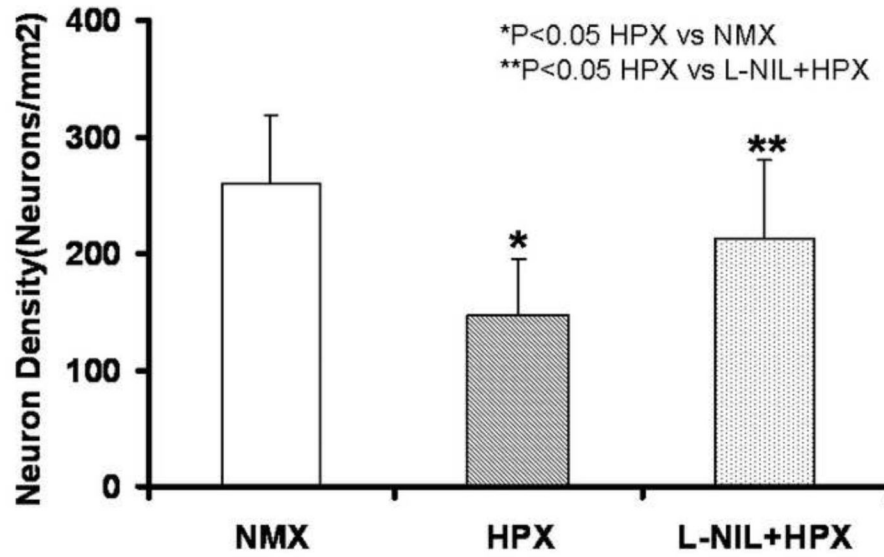


Figure 12. L-NIL Prevents Neuronal Loss in Fetal Hippocampus During Chronic Hypoxia
The impact of L-NIL on neuronal loss during chronic fetal hypoxia is illustrated here for hippocampus. Neural cell density is expressed as the total Nissl staining cells/ mm². L-NIL essentially eliminated neuronal loss secondary to chronic hypoxia.

Table 1

Antibodies Species and Dilution Factors Information

| Application | Primary Antibodies | Species | Dilution | Secondary Antibodies |
|----------------------|------------------------------------|---------|----------|-------------------------------------|
| Injury Index Mapping | Anti-GFAP (Sigma) | Mouse | 100 | Universal LSAB + System-HRP (DAKO) |
| | Anti-ATF3 (Sigma) | Mouse | 50 | Universal LSAB + System-HRP (DAKO) |
| ATF3 Co-localization | Anti-ATF3 (Sigma) | Rabbit | 200 | Donkey anti rabbit + FITC (Jackson) |
| | Anti-GFAP (Sigma) | Mouse | 500 | Donkey anti mouse + Red-X (Jackson) |
| | Anti- β -Tubulin III (Sigma) | Mouse | 1000 | Donkey anti mouse + Red-X (Jackson) |
| NOSs Co-localization | Anti-iNOS (BD bioscience) | Mouse | 200 | Donkey anti mouse + Red-X (Jackson) |
| | Anti-ATF3 (Sigma) | Rabbit | 200 | Donkey anti rabbit + FITC (Jackson) |
| | Anti-GFAP (Sigma) | Rabbit | 200 | Donkey anti rabbit + FITC (Jackson) |
| | Anti-nNOS (Cell signaling) | Rabbit | 100 | Donkey anti rabbit + FITC (Jackson) |
| | Anti-ATF3 (Sigma) | Mouse | 200 | Donkey anti mouse + Red-X (Jackson) |
| | Anti-GFAP (Sigma) | Mouse | 500 | Donkey anti mouse + Red-X (Jackson) |

Table 2

Chronic Hypoxia Induces Fetal Brain Injury in Selected Areas

| Brain Structure | Nuclei | Injury Indexes | | |
|---------------------|--------------------------|----------------|-------|-------|
| | | ATF3 | GFAP | TUNEL |
| Cerebral cortex | Global wide | ++ | ++ | ++ |
| | cingulum | - | +++++ | - |
| Hippocampal region | orices layer hippocampus | +++ | +++ | +++ |
| | CA1 | + | + | + |
| | CA2 | + | + | + |
| | CA3 | ++++ | ++++ | ++++ |
| Thalamic nuclei | laterodorsal thal nu | ++ | ++ | ++ |
| | post thalamic nu | + | + | + |
| | ventrol thalamic nu | ++ | ++ | ++ |
| | paraventricular thal nu | + | + | + |
| | mediodorsal thal nu | + | + | + |
| | central thalamic nu | ++ | ++ | ++ |
| | reuniens thalamic nu | +++ | +++ | +++ |
| | others | - | - | - |
| Hypothalamic nuclei | dorsomed hypothal nu | + | + | + |
| | ventromed hypothal nu | + | + | + |
| | lat hypothal | + | + | + |
| | others | + | + | + |